Remote sensing for evaluating crop water stress at field scale using infra-red thermography: potential and limitations

Saleh Taghvaeian[1] and José L. Chávez
Civil & Environmental Engineering Department, Colorado State University, Fort Collins, CO

Jon Altenhofen
Northern Colorado Water Conservancy District, Berthoud, CO

Tom Trout and Kendall DeJonge
Water Management Research Unit, USDA-Agricultural Research Service, Fort Collins, CO

Abstract. Over the past few decades, the competition for freshwater resources has substantially increased in arid/semi-arid areas, exacerbating the pressure on the largest user of water, namely agriculture, to consume less water. However, reducing crop consumptive water use or evapotranspiration through water stress can have a negative impact on production economics if not precisely managed. Remote sensing of crop canopy temperature is a scientifically-based and easy-to-apply method that can be used at field scales to evaluate crop water status at or near real-time. In this study, thermal images of maize canopy under two deficit irrigation regimes were acquired using a hand-held thermal camera. The results showed that the low-frequency deficit irrigation treatment resulted in higher maize temperatures compared to the high-frequency deficit irrigation regime. A methodology for converting the temperature value of each pixel into a spatially variable crop water stress index (CWSI) is described. Within the low-frequency deficit irrigation treatment, estimated CWSI values were correlated with spatial variations in soil texture. Finally, the potential of infrared thermography and current limitations are discussed in detail.

1. Introduction

Historically, irrigated agriculture has been the largest user of freshwater resources in arid/semi-arid areas such as the Western United State. This sector, however, has recently been under escalating pressure from other growing users (e.g. urban municipalities, oil and gas industry, environmental-in-stream flows) to reduce its water use. In addition, the predicted increase in frequency and intensity of droughts under a changing climate poses a separate and perhaps less-understood threat to irrigated agriculture. Hence, it seems that agricultural activities in arid/semi-arid regions inevitably need to adopt new irrigation management strategies that could secure their sustainable existence in the future. One of these new strategies is deficit (or regulated, limited) irrigation, which offers a great potential in terms of reducing inputs and increasing water productivity (English and Raja 1996). Compared to traditional full irrigation approaches, deficit irrigation practices should be managed more precisely since the crops are being allowed to experience some degree of water stress (Mahan et al. 2012), and management of historical return flows (deep percolation and runoff) must be considered. Thus, it is of crucial importance for farmers and irri-

[1] Civil and Environmental Engineering Department
Colorado State University
1372 Campus Delivery
Fort Collins, CO 80523-1372
Tel: (970) 491-3381
e-mail: saleh.taghvaeian@colostate.edu

gation managers to closely and accurately monitor stress development in order to apply water before the experienced stress intensifies to levels higher than the target level. Previous studies have shown that infrared thermography can serve as an effective tool in evaluating crop water status of several agricultural and horticultural crops, such as sunflower (Hashimoto et al. 1984), muskmelon (Clarke 1997), maize (Liu et al. 2011, Zia et al. 2011), soybean and cotton (O'Shaughnessy et al. 2011), winter wheat (Zia et al. 2012), grapevine (Jones et al. 2002, Grant et al. 2007, Möller et al. 2007), persimmon and citrus trees (Jiménez-Bello et al. 2011), and palm trees (Cohen et al. 2012).

The effectiveness of remote sensing of canopy temperature lies in the fact that the presence of water stress corresponds with a closure of stomata and a decrease in the transpiration rate, which is the main process responsible for cooling the plants, with a resulting increase in canopy temperature. However, crop temperature is sensitive to other variables, such as air temperature, relative humidity, wind speed, and incoming irradiance. Thus, most of the mentioned studies have implemented methods to minimize the effect of these environmental variables. One method that has been used successfully is the Crop Water Stress Index (CWSI), which normalizes the actual canopy temperature using empirically (Idso et al. 1981) or theoretically (Jackson et al. 1981) derived maximum and minimum limits of temperature differences (between the plant and the air) that can be possibly reached for a particular region (based on climatic conditions) and for the crop under consideration. The value of CWSI can range between zero and unity, representing the non-water-stressed and water stressed (non-transpiring) conditions, respectively. The objectives of the present experiment were two-fold:

- To identify the potential and limitations of using an affordable handheld thermal camera to detect the effect of deficit irrigation on maize temperature at field scale; and,
- To estimate maize CWSI based on the acquired thermal images.

2. Methods

This experiment was conducted on a research farm that was located near the city of Greeley in Northern Colorado (Lat. 40º 26.647’ N, Long. 104º 38.100’ W, Alt. 1425 m). The soil texture was fairly heterogeneous, ranging from loamy sand to clay loam. Maize (*Zea mays* L.) for grain yield was planted in this field on May 2, 2012 under three irrigation treatments: well irrigated, high-frequency deficit irrigated (HFDI), and low-frequency deficit irrigated (LFDI). The focus of this study, however, was on the ability of thermal imagery to capture any variations in canopy temperature between the two latter treatments (HFDI and LFDI). The HFDI received a total of seven irrigations during the growing season with an average net depth (applied minus surface runoff) of 42 mm, while the LFDI received only three irrigations with average net depth of 267 mm. These deficit irrigation treatments were designed to meet two different goals: minimizing (in case of HFDI) versus maintaining (in case of LFDI) adequate deep percolation to maintain groundwater levels and irrigation return flows while for both treatments trying to maximize water productivity and grain yields.

2.1. Canopy temperature

A ground-based, handheld FLIR camera (model E30, FLIR Systems, Inc., Wilsonville, Oregon, USA) was used to take canopy thermal images. This model has a size of

246×97×184 mm (L×W×H) and weighs 0.825 kg with the battery installed. The built-in sensor is a thermal detector (microbolometer), thus it does not require an external cooling system. This sensor is sensitive to thermal radiation in the 7.5-13.0 μm range of the electromagnetic spectrum, which is wider than the 10.4-12.5 μm range of the sensor onboard Landsat TM and ETM+ and some infrared thermometers. The reported accuracy is ±2.0 ˚C for target temperatures varying from -20 to 120 ˚C. Despite the fairly small number of pixels per image (160×120 pixels), this model has several features that are advantageous in field applications, such as its light weight, a large (90 mm) touch screen display, the ability to adjust the assumed emissivity of the surface (or target), and the inclusion of a visible light camera. Maize canopy thermal images were taken from the top of a 3.0-m tall ladder on four dates during the 2012 growing season: Jul 19, Jul 26, Aug 9, and Sep 5. Maize growth stage changed from V15 to R6 during this period. Maximum canopy cover had been reached by Jul 19 in both treatments. The image acquisition time varied from 13:15 to 14:10 MST (Mountain Standard Time), always after the local solar noon (around 12:00 MST).

2.2. Crop water stress index

Estimation of crop water stress index (CWSI) needed to be performed using different software packages, since the FLIR software (FLIR Tools, version 2.2) did not support any image processing. In this study, the acquired thermal images were first saved in 8-bit grayscale, uncompressed TIFF format and then opened in ArcGIS 10.0 environment. Next, the digital number of each pixel was converted back to the temperature using the equation provided in Cohen et al. (2005):

$$T_{(x,y)} = T_{\min} + \frac{DN_{(x,y)}}{255} \cdot T_{span} \quad (1)$$

where $T_{(x, y)}$ is the calculated temperature of pixel (x, y), T_{min} is the minimum temperature of the image before saving it in TIFF format, $DN_{(x, y)}$ is the digital number (gray level) of pixel (x, y) in the TIFF image, 255 is the maximum number of gray levels in a 8-bit image, and T_{span} is the range of temperatures before saving the image in TIFF format.

Finally, the CWSI was estimated on a spatially distributed basis. The computation of CWSI was based on the empirical approach of Idso et al. (1981), since this approach is simple to apply and it only requires air temperature and relative humidity data. These two variables were measured continuously at the study site and averaged and stored every 5 minutes using a data-logger (model CR1000, Campbell Scientific Inc., Logan, Utah, USA). The required upper and lower limits of canopy-air temperature differential were identified based on the empirical non-water-stressed and non-transpiring baselines developed by Taghvaeian et al. (2012a):

$$dT_{LL} = 2.73 - 1.90 \cdot VPD \quad (2)$$

$$dT_{UL} = 2.73 - 1.90 \cdot VPG \quad (3)$$

where VPD is vapor pressure deficit and VPG is vapor pressure gradient. The above equations were developed for maize in Northeastern Colorado, with agro-climatological conditions that were very similar to those of this study in Northern Colorado. Since the diurnal curve of canopy temperature has a peak about one to two hours after the solar noon and because thermal images were acquired within the same period, estimated CWSI values are expected to represent the largest values that can be obtained during each day. For winter wheat, Zia et al. (2012) acquired hourly thermal images during the day and found that

CWSI was largest during the 13:00 to 14:00 hours. Similar results have been reported for CWSI based on thermometry data (Irmak et al. 2000).

3. Results and discussion

3.1. Canopy temperature

Figure 1 presents visible and thermal images acquired by the FLIR handheld camera on four dates during the growing season. The camera was pointing due North with the image centerline being aligned with treatment's border, so that the LFDI is on the left and the HFDI is on the right side of each image. The centerline can be easily identified in each thermal image of Figure 1 due to the higher temperature of the exposed underlying soil. In addition, the two maize rows in the middle of the image were not irrigated, so they usually had a higher temperature than the treatments surrounding.

The first image was taken on Jul 19, about 15 and 2 days after the last previous irrigation of LFDI and HFDI treatments, respectively. Thus, the condition at HFDI was at or near non-water-stressed. According to the thermal image, the majority of maize plants in this treatment had a temperature range of 27-30 ˚C, while the range was about 29-32 ˚C for the LFDI treatment. This is similar to the results of Zia et al. (2011) who observed 2.2 and 2.9 ˚C difference in the temperature of two maize verities that were not irrigated for 14 days, compared to well-irrigated treatments. The temperature of the exposed soil reached up to 58 ˚C, which shows that the background soil can have a significant contribution to detected temperature if it is observed by the remote sensing sensor.

The next image acquisition occurred on Jul 26. The HFDI was irrigated one day earlier, while the LFDI had not received any additional irrigation (22 days passed since the last previous irrigation). Soil temperature reached 56 ˚C on this date. The range of temperatures did not change significantly compared to the first date. However, the distribution of values shifted toward the upper ends of the ranges (30 ˚C for HFDI and 32 ˚C for LFDI). It should be noted that despite the similarity in canopy temperature ranges, air temperature was 4 ˚C cooler on Jul 26. In other words, detected canopy temperatures may have been higher if the air temperature had been similar to that of Jul 19.

On the third date (Aug 9), most of the pixels that fell within the HFDI had temperatures varying from 30 to 32 ˚C. This date was 5 days after the HFDI received 36 mm of net irrigation depth. The portion of the LFDI that was captured in the thermal image had still not received any irrigation, so the higher plant temperatures (32-34 ˚C) were expected. Maximum detected soil temperature was about 54 ˚C on this date. Finally, the last thermal image was taken on Sep 5, which corresponded to the R6 growth stage of maize. The range of detected temperatures was similar to the range obtained on the third date, with changes in the distribution of values. However, this date was the coolest date among the four days with an air temperature of 27.4 ˚C at the image acquisition time. Soil temperature reached 51 ˚C on this date.

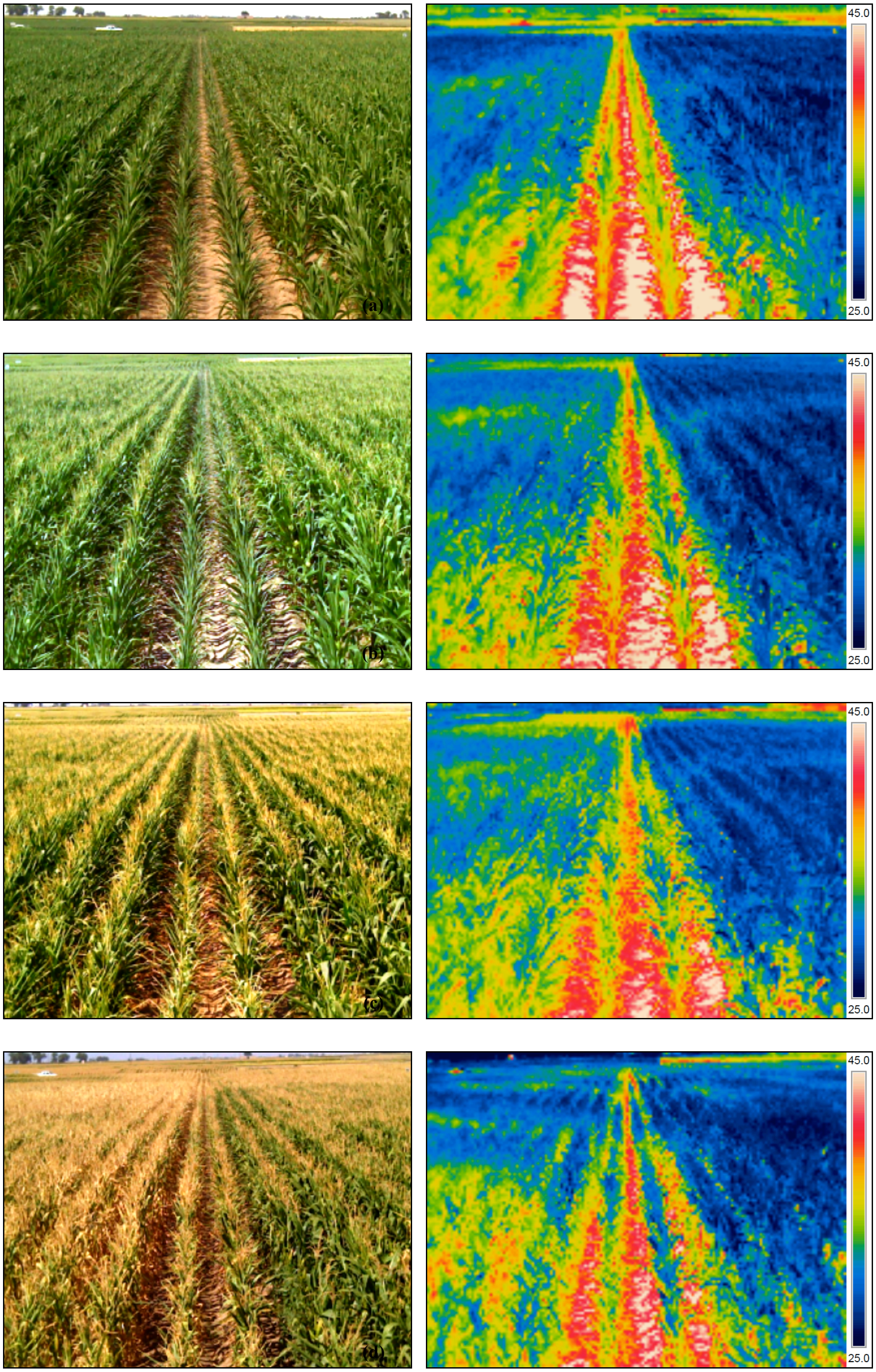

Figure 1. Thermal and visible images taken by the handheld camera on (a) Jul 19; (b) Jul 26; (c) Aug 9; and, (d) Sep 5, 2012. The legends on the right side of the thermal images represent temperature color ramp in ˚C. Left of images indicates LFDI, right of images indicates HDFI, and two center rows are borders.

3.2. A close-distance look at maize

Thermal cameras provide the opportunity to evaluate the temperature variations in crop canopies as affected by factors such as sun illumination. Figure 2 depicts a close-distance image of maize, containing different plant parts such as stalk, leaf, and ear. According to this image, the temperature difference between sunlit and shaded parts of the leaf reached 5 ˚C. Jones et al. (2002) observed an average 3 ˚C difference between sunlit and shaded leaves of grapevine. They also found that the leaf temperature sensitivity to stomatal conductance was significantly larger for sunlit leaves in comparison to the shaded ones and suggested to exclude shaded leaves from the analysis. The empirical CWSI method of Idso et al. (1981) should also be applied using the temperature data of a sunlit canopy. Hence, it seems that the data collection configuration followed in this study, which is acquiring imagery close to solar noon with camera pointing toward North, can be recommended for regular applications of thermography in crop water status evaluation.

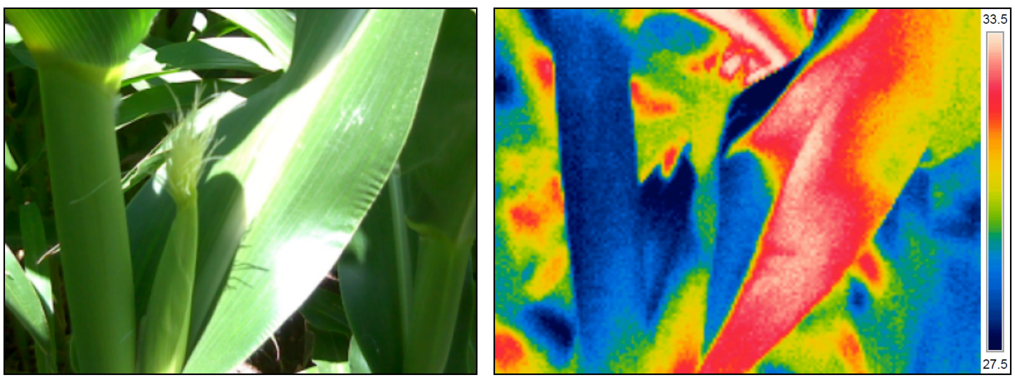

Figure 2. Close-distance visible and thermal images containing different plant parts under sunlit and shaded conditions.

Another observation in the close-distance image (Figure 2) is the radial distortion that can be identified by comparing the straightness of maize stalk between thermal and visible images. Luhmann et al. (2010) performed a test on four handheld cameras, including two FLIR models (InfraCam and B200), and found that all acquired images had a fairly large geometric distortion. This problem needs to be resolved if the thermal and visible images need to be co-registered for further image processing. However, it would not pose a significant challenge if the thermal image is going to be used alone for purposes such as estimating the crop water stress index.

3.3. Crop water stress index

As expected, the difference between treatments and dates was better depicted after converting thermal images into CWSI maps (Figure 3). On Jul 19 (Figure 3a), most of the HFDI and parts of the LFDI were under minimal water stress. The rest of the pixels had a range of CWSI that was mainly from 0.2 to 0.4 (or 20 to 40% water stress). The range of CWSI for the two dryland rows in the middle was 0.3-0.6. The stress severity increased for both treatments on Jul 26 (Figure 3b), but the magnitude of this increase was larger for the LFDI. The CWSI variability within this treatment was also very interesting. While some plants showed almost no signs of stress, other parts of the LFDI treatment reached a maximum CWSI limit of unity (100 % stress). A closer investigation revealed that the observed

CWSI variability was consistent with the variability in soil texture. Maize plants in coarser-textured soil were at a higher level of stress, while those in the finer-textured soil remained at lower levels of water stress. This is mainly due to the fact that fine-textured soils have a larger water holding capacity, a characteristic that makes them more suitable for practicing low frequency deficit irrigation. Water stress severity was fairly similar on Aug 9 (Figure 3c) for HFDI, but it increased for LFDI. On this date, only a few pixels in LFDI had a minimum CWSI. Stress severity was largest on the last date (Sep 5, Figure 3d), but this was more due to the crop senescence rather than water stress.

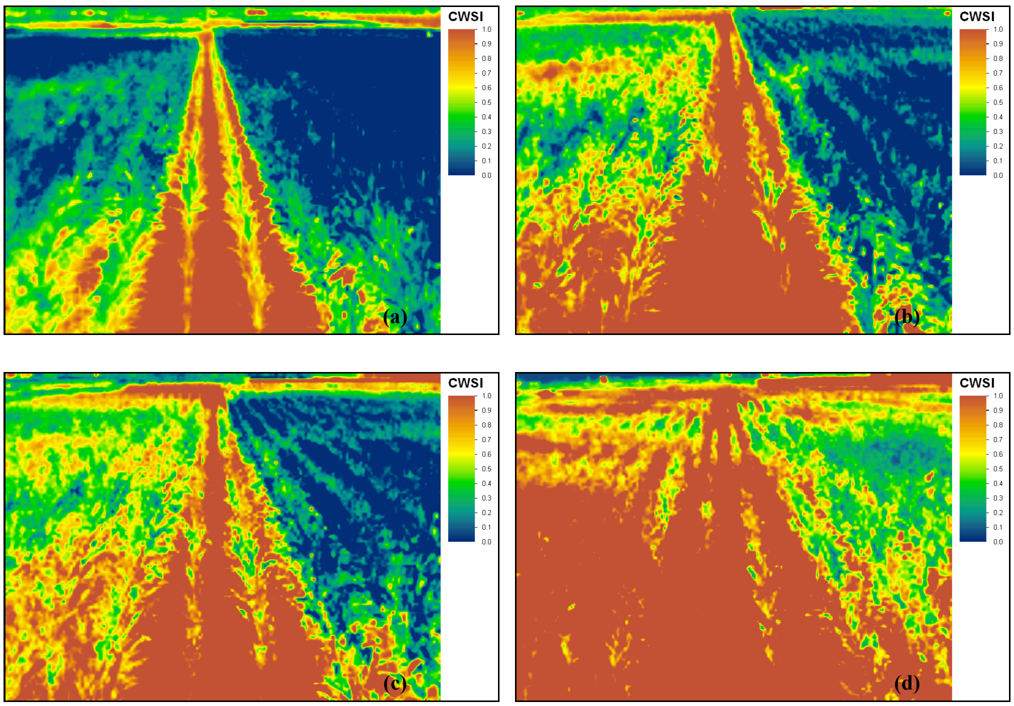

Figure 3. Maize CWSI estimated based on the thermal images acquired on (a) Jul 19; (b) Jul 26; (c) Aug 9; and, (d) Sep 5, 2012.

It is worth mentioning that CWSI values were estimated using non-water-stressed and non-transpiring baselines that were developed in Northeastern Colorado, based on the data collected by infrared thermometers (model SI121, Apogee Instruments, Inc., Logan, Utah, USA). Due to the close proximity, development and application sites had similar climatic conditions. So a major source of variation in baselines was eliminated, as previous studies have shown that baselines are fairly transferable within the boundaries of each climatic region (Taghvaeian et al. 2012a,b). However, the intrinsic difference between thermometry and thermography and the effect it may have had on the results should be acknowledged. For example, the thermometer readings used in baseline development were integrated over sunlit and shaded plant parts, while thermal images in this study differentiated these components. Thus, there seems to be the need to develop specific baselines that could be used for analyzing thermal imagery. For sunflower, Nielsen (1994) found that non-water-stressed baselines developed using leaf versus canopy temperatures had slightly different slopes and intercepts.

3.4. Potential and limitations

The results of this study confirm previous findings that infrared thermography offers great potential in evaluating water stress level in crop communities at or near real-time. Compared to thermometry, which yields only one averaged value, thermal images provide a temperature value for all of the pixels within the sensor's field of view. Thus, it is sometimes easier to differentiate between different components, such as sunlit versus shaded plant parts and wet versus dry soil surfaces. Thermal cameras are not complicated devices and can be used by farmers for improving irrigation scheduling under water limitations. However, the available thermal cameras are mainly designed for non-agricultural uses, such as building and machinery inspection. As a result, the included features and abilities are designed to better serve these types of applications. A wide-spread use of thermography by farmers may provide incentive for manufacturers to develop modified cameras that are more appropriate for agricultural applications. One simple modification may be to add the ability of converting the thermal image into a CWSI image, using basic input data entered by the user (climatic region, crop type, air temperature, and relative humidity).

The most hindering drawback of the thermal camera, and its accompanying software, that were used in this experiment was their limited ability in performing image processing analysis. For example, the ability to co-register visible and thermal images offers a lot of potential in obtaining temperature statistics for each component of interest (e.g. plant, soil, etc.). However, performing the co-registration could not be accomplished due to two factors: *i)* the visible light camera had a field of view that was approximately two times larger than that of the thermal camera; and, *ii)* the radial distortion was significant in the thermal image. In addition, the provided software did not allow saving the thermal images in any image or text formats. The only option was to generate PDF reports and then use the "Take a snapshot" option of Adobe Reader to capture the thermal image in a favorable format. These issues mainly limit the use of this thermal camera for research applications, but another limitation causes inconveniences for practical applications. This limitation was in report generating ability of the provided software. While FLIR Tools allows the user to generate reports and to save them in PDF format, it is not possible to edit generated reports at a later time. So if the user realizes that a comprehensive report he/she prepared has some minor errors, the entire report needs to be produced from scratch.

Despite these limitations, it should be mentioned that the relatively low cost of the thermal camera used in this study (USD 3000, purchased in June 2012) most probably outweighs the mentioned limitations, especially if the camera will be used by water managers for routine irrigation management. Advanced models of FLIR cameras and processing software packages have eliminated some of these limitations, at a cost of higher purchasing price. Figure 4 demonstrates visible and thermal images acquired over other crops. The top two images show an onion field at early growth stages under furrow irrigation system. The bottom images show a cabbage field that is being irrigated by a sprinkler irrigation system (center pivot). Unlike visible images, the thermal images allow the detection of irrigated areas due to their lower temperatures. The thermal image of the center pivot system also provides an insight into another application of thermography in agriculture, which is to monitor the performance of agricultural machinery.

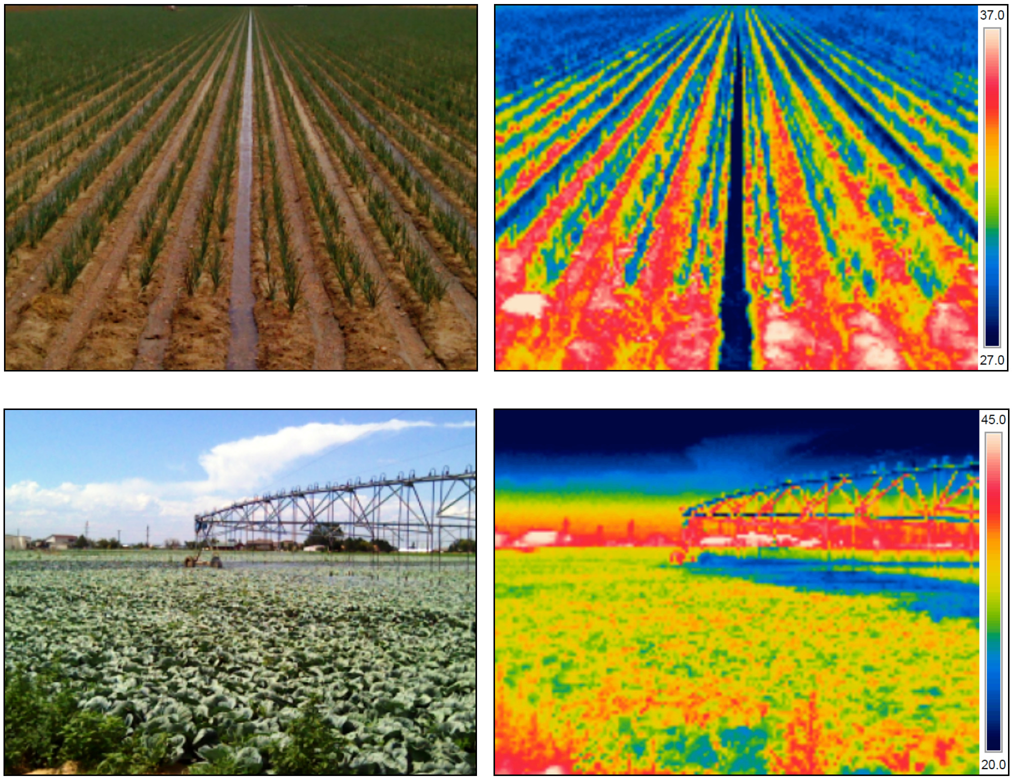

Figure 4. Application of the FLIR handheld camera for monitoring the temperature of other crops: onion (top) and cabbage (bottom). The legends on the right side of the thermal images represent temperature color ramp in ˚C.

4. Conclusions

A handheld thermal camera was used to detect the temperature of maize canopies in Northern Colorado, USA, under two different deficit irrigation treatments: low frequency (LFDI) and high frequency (HFDI). The results showed that the two treatments had significantly different temperatures, suggesting that crop thermography can be an effective tool in practicing canopy temperature-based irrigation scheduling. The exposed sunlit soil had temperatures that were more than 20 ˚C higher than that of maize canopy. This observation renders a major advantage of thermography methods over thermometry approaches, which is their ability to provide useful information even when the underlying soil is viewed by the sensor. In thermometry methods, the sensor installation height and the look and view angles should be carefully identified in order to avoid viewing any underlying soil. However, obtaining a pure-canopy reading may not be possible at all at early stages of growth, when the emerging crop only covers a small fraction of soil surface. Another advantage of thermography over thermometry is differentiating between sunlit and shaded leaves where sunlit will show greater water stress and higher temperatures under deficit conditions.

Applying the empirical crop water stress index (CWSI) method improved the presentation of stress level differences between LFDI and HFDI, as it eliminated the effects of environmental variables. The variability in CWSI within LFDI treatment was correlated with the variability of soil texture. Areas with a coarser texture and a lower water holding capacity had a higher CWSI value and *vice-versa*. This finding reveals that thermal images can also be used by farmers to obtain detailed information about the spatial variability in physical characteristics of their soils and potential impact of water stress. In addition, thermal images may provide useful information on the presence and distribution of other abiotic, and even biotic, stress factors.

Acknowledgements. This experiment was financially supported by the Regenesis Management Group. The funding to purchase the thermal camera was provided by the Northern Colorado Water Conservancy District. The agronomic field work and irrigations were done by the USDA-ARS Water Management Research Unit.

References

Clarke, T. R. 1997: An empirical approach for detecting crop water stress using multispectral airborne sensors. *HortTechnology*, **7**(1), 9-16.

Cohen, Y., Alchanatis, V., Meron, M., Saranga, Y., and J. Tsipris, 2005: Estimation of leaf water potential by thermal imagery and spatial analysis. *J. Exp. Bot.*, **56**(417), 1843-1852.

Cohen, Y., Alchanatis, V., Prigojin, A., Levi, A., Soroker, V., and Y. Cohen, 2012: Use of aerial thermal imaging to estimate water status of palm trees. *Precision Agric.*, **13**(1), 123-140.

English, M., and S. N. Raja, 1996: Perspectives on deficit irrigation. *Agric. Water Manage.*, **32**,1-14.

Grant, O. M., Tronina, L., Jones, H. G., and M. M. Chaves, 2007: Exploring thermal imaging variables for the detection of stress responses in grapevine under different irrigation regimes. *J. Exp. Bot.*, **58**(4), 815-825.

Hashimoto, Y., Ino, T., Kramer, P. J., Naylor, A. W., and B. R. Strain, 1984: Dynamic analysis of water stress of sunflower leaves by means of a thermal image processing system. *Plant Physiol.*, **76**, 266-269.

Idso, S. B., Jackson, R. D., Pinter Jr., P. J., Reginato, R. J., and J. L. Hatfield, 1981: Normalizing the stress-degree-day parameter for environmental variability. *Agric. Meteorol.*, **24**(1), 45-55.

Irmak, S., Haman, D. Z., and R. Bastug, 2000: Corn: Determination of crop water stress index for irrigation timing and yield estimation of corn. *Agron. J.*, **92**, 1221-1227.

Jackson, R. D., Idso, S. B., and R. J. Reginato, 1981: Canopy temperature as a crop water stress indicator. *Water Resour. Res.*, **17**(4), 1133-1138.

Jiménez-Bello, M. A., Ballester, C., Castel, J. R., and D.S. Intrigliolo, 2011: Development and validation of an automatic thermal imaging process for assessing plant water status. *Agric. Water Manag.*, **98**(10), 1497-1504.

Jones, H. G., Stoll, M., Santos, T., de Sousa, C., Chaves, M. M., and O. M. Grant, 2002: Use of infrared thermography for monitoring stomatal closure in the field: application to grapevine. *J. Exp. Bot.*, **53**(378), 2249-2260.

Liu, Y., Subhash, C., Yan, J., Song, C., Zhao, J., and J. Li, 2011: Maize leaf temperature responses to drought: Thermal imaging and quantitative trait loci (QTL) mapping. *Environ. Exp. Bot.*, **71**(2), 158-165.

Luhmann, T., Ohm, J., Piechel, J., and T. Roelfs, 2010: Geometric calibration of thermographic cameras. In: Proceedings of the ISPRS Commission V Mid-Term Symposium Close Range Image Measurement Techniques, 21-24 June 2010, Newcastle upon Tyne, United Kingdom, Mills, J. P., Barber, D. M., Miller, P.E. and I. Newton, (Eds), 411-416.

Mahan, J. R., Young, A. W., and P. Payton, 2012: Deficit irrigation in a production setting: canopy temperature as an adjunct to ET estimates. *Irrig. Sci.*, **30**,127-137.

Möller, M., Alchanatis, V., Cohen, Y., Meron, M., Tsipris, J., Naor, A., Ostrovsky, V., Sprintsin, M., and S. Cohen, 2007: Use of thermal and visible imagery for estimating crop water status of irrigated grapevine. *J. Exp. Bot.*, **58**(4), 827-838.

Nielsen, D. C. 1994: Non water-stressed baselines for sunflowers. *Agric. Water Manag.*, **26**(4), 265-276.

O'Shaughnessy, S. A., Evett, S. R., Colaizzi, P. D., and T. A. Howell, 2011: Using radiation thermography and thermometry to evaluate crop water stress in soybean and cotton. *Agric. Water Manag.*, **98**(10), 1523-1535.

Taghvaeian, S., Chávez, J. L., and N. C. Hansen, 2012a: Infrared thermometry to estimate crop water stress index and water use of irrigated maize in Northeastern Colorado. *Remote Sens.*, **4**(11), 3619-3637.

Taghvaeian, S., Chávez, J. L., and N. C. Hansen, 2012b: Ground-based remote sensing of corn evapotranspiration under limited irrigation practices. In: Proceedings of the 32nd Annual American Geophysical Union Hydrology Days, March 21-23, 2012, Fort Collins, CO, USA, 119-131.

Zia, S., Sophrer, K., Wenyong, D., Spreer, W., Romano, G., Xiongkui, H., and J. Müller, 2011: Monitoring physiological responses to water stress in two maize varieties by infrared thermography. *Int. J. Agric. Biol. Eng.*, **4**(3), 7-15.

Zia, S., Wenyong, D., Spreer, W., Sophrer, K., Xiongkui, H., and J. Müller, 2012: Assessing crop water stress of winter wheat by thermography under different irrigation regimes in North China Plain. *Int. J. Agric. Biol. Eng.*, **5**(3), 24-34.